A preliminary study on an optical system for nautical and maritime traffic monitoring

2021 International Workshop on Metrology for the Sea; Learning to Measure Sea Health Parameters (MetroSea) | 978-1-6654-1458-6/21/$31.00 ©2021 IEEE | DOI: 10.1109/MetroSea52177.2021.9611575

Silvio Del Pizzo
Department of Sciences and Technologies
University of Naples "Parthenope"
Naples, Italy
silvio.delpizzo@uniparthenope.it

Salvatore Troisi
Department of Sciences and Technologies
University of Naples "Parthenope"
Naples, Italy
salvatore.troisi@uniparthenope.it

Antonio Angrisano
Department of Engeenering
Messina University
Messina, Italy
antonio.angrisano@unime.it

Fabiana Di Ciaccio
Department of Sciences and Technologies
University of Naples "Parthenope"
Naples, Italy
fabiana.diciaccio@uniparthenope.it

Salvatore Gaglione
Department of Sciences and Technologies
University of Naples "Parthenope"
Naples, Italy
salvatore.gaglione@uniparthenope.it

***Abstract*— The nautical traffic is very difficult to monitor since many vessels are not cooperative. VTSs (Vessel Traffic Systems) use several sources of information for estimating ships' Position Navigation and Velocity, such as AIS (Automatic Identification System) and RADAR (RAdio Detection And Ranging); nevertheless, VTS areas do not cover the entire costal area of a country. In many cases the classification and identification of small non-AIS vessels could provide an important to the safety of navigation.**

Indeed, especially during the summer, the nautical tourism has a great impact on the maritime traffic congestion. The issue involves many institutions such as Marine Protected Areas (MPAs) and local maritime authorities which are not able to monitor the high volume of nautical traffic. This work introduces an optical system designed to monitor the traffic in small coastal areas based on images acquired by a single camera. The reliability and accuracy of the system is conditioned by the size of the pixel on the sea surface (Ground Sample Distance - GSD) and by the camera footprint area as well. More in detail, this work focuses on the detection of the best camera placement on the coast for optimizing the GSD size and obtaining the shape of camera footprint. The inspection was conducted on a target area of the MPA "Punta Campanella" located on the Sorrento coast.

Keywords—Metrology-Photogrammetry-Maritime Traffic Monitoring -Low cost- Positioning-Navigation

I. Introduction & Motivations

The maritime traffic management has always been a challenging task for the international maritime community, countries and local maritime authorities [1], being fundamental for both safety and security purposes [2-4]. Generally, all the ships find their own way and conflicts are resolved locally in according to the COLREGs (Convention on the International Regulations for Preventing Collisions at Sea) [5]. In some areas characterized by high-density traffic, the IMO (International Maritime Organization) and the maritime authorities tackled this problem introducing the *Ships Routeing* such as Traffic Separation Schemes (TSS), recommended routes, precautionary areas and traffic lanes [6,7].

Traditionally, the master of a ship is responsible for the vessel's course and speed and can be assisted by a pilot where necessary [8]. In 2000 a new SOLAS issue came into force, the IMO recognizes a significant role to the VTS (Vessel Traffic Services). These shore-side systems provide important information on weather hazard, warnings, traffic data to all the ships navigating in their operational area [9]. The VTS Control Center manages all this information and it tracks the vessel traffic on its operational area. Moreover, the VTS operator may directly contact the ship in case of a risk of collision, accident or other events that could create traffic congestion as well as an environmental hazard. For this reason, when a ship enters in a VTS area it must contact the control center, usually by radio and maintaining an active communication via a VHF radio channel [10]. The Governments establish the number and the size of VTS area according to the volume of traffic or the degree of risk [11].

The above-mentioned procedures do not involve all types of ships; in Italy the collaboration with a VTS is in fact mandatory for all the ships over 300 GT (Gross Tonnage), all the passengers and fishing ships as well as, recreational boats with a minimum length of 45 meters. Furthermore, the VTS areas do not entirely cover the Italian coasts, since they have been established only for the main ports of the country.

The vessel traffic volume can be estimated using web services like Marine Traffic©, that records the tracks of the ships equipped with AIS (Automatic Identification System) [12,13]. There are no in-depth studies on the volume of nautical traffic of pleasure boats, although in 2018 almost five hundred accidents involved these type of vessels as recorded by the Italian Department for Transport and Navigation [14]. However, recreational craft tracking, and monitoring is still an ongoing challenge, especially because these vessels are not cooperative. This becomes particularly evident during the summer, when the nautical tourism heavily impacts on the maritime traffic along the Italian coasts.

This phenomenon creates several problems to the marine environment [15,16], and to the coastal erosion [17,18].

Marine Protected Areas (MPAs) have been established to preserve the marine environment and its biodiversity by identifying a spatially delimited areas where any kind of human activity is limited. The Italian Ministry of the Environment and Protection of Land and Sea establishes the overall area assigned to a generic MPA; this area is divided in three zones named A-B-C in which different environmental protection regimes are applied:

- **Zone A** defines an integral reserve area, where only scientific research and authorized diving are allowed. The nautical traffic is here prohibited regardless of the vehicle's propeller.
- **Zone B** defines a general reserve area, where the anchorage is not allowed but it is possible to navigate with limited speed; in some sub-areas the use of specific propellers can be forbidden.
- **Zone C:** defines a partial reserve area, where the nautical traffic as well as the anchorage are allowed, but with speed limitations.

The Coast Guard encounters many difficulties in monitoring the nautical traffic, especially when it comes to the speed or the compliance of no-go areas.

This paper describes a preliminary study of a monitoring system based on smart surveillance cameras able to identify recreative boats or vessels, tracking them and estimate their position and speed. This system could help the Coast Guard to detect any misbehaviour of craft conductors: it could in fact be employed to estimate the nautical traffic density over specific areas as it works on non-cooperative vessels.

In this study different geomatic techniques (GIS & Photogrammetry) are exploited to estimate the best location for the installation of a smart camera, based on the potential size of GSD (Ground Sample Distance). This latter parameter will be taken as reference for estimating the potential accuracy of the system in terms of speed and position detection.

The paper is organized as follows: section 2 presents the theoretical background and a brief description of the analysed MPA while in section 3 the obtained results and their discussion are reported. Finally, section 4 illustrates the conclusions and some future developments.

II. Background

A. Case study

The study was conducted on the specific no-go area of the MPA "Punta Campanella". The MPA is located at the south-western end of the Sorrentine Peninsula, part of the territory of the municipality of Massa Lubrense (Metropolitan City of Naples), in the Campania region of Italy. The reserve includes the coast that extends for 30 Km from Punta del Capo (Gulf of Naples) to Punta Germano (Gulf of Salerno) and includes a charming succession of grottoes, inlets, and bays. A few miles off the coast, small reefs are scattered here and there (Vervece, Vetara, Isca and Li Galli). Specifically, the study focuses its inspection on the Vervece integral reserve area, bounded by four yellow buoys whose geographic coordinates are linked to the ED50 reference system as well as reported on the MPA regulation.

B. Theoretical Background

An optical monitoring system is designed to maximize the coverage area and increase the measurement performances as well. The choice of the camera position and orientation plays a fundamental role in achieving such goal. This section describes the methodology developed to locate and direct a generic camera, with the aim of minimizing the mean GSD dimension.

The camera position will surely be constrained to the coast surface of the area of interest. For this reason, a DSM (Digital Surface Model) was employed to detect the points which could best fits, for a specific camera, the installation on the coastal surface.

A finite pinhole camera model [19] with specific sensor size and focal length is here considered. The camera coordinate system has its origin in the optical centre of the camera, while the three axes can be set basing on the user's scope. In this case, the z-axis is defined to coincide with the camera optical axis positive towards the view direction, while the x- and y-axes are parallel to the columns and rows of pixels in the image plane.

The proposed approach is based on the single-view geometry, a well-known configuration in Photogrammetry and in Computer Vision fields [20-21]. This configuration is employed for measurements purposes in multiple fields, such as: player tracking during sport events [22-23], controlling jet flow [24], navigation [25-26], vehicle attitude estimation [27-28] and object 3D reconstruction [29].

A generic point in the 3D space with coordinates $\mathbf{X} = [\mathrm{X}, \mathrm{Y}, \mathrm{Z}]$ is mapped to the point on the image plane with coordinates $\mathbf{x} = [x, y]$; this latter is created by the intersection between a line, joining the point $\mathbf{X}$ to the optical centre $\mathbf{C} = [\mathrm{Xc}, \mathrm{Yc}, \mathrm{Zc}]$, and the image plane [30]. If both coordinates systems are expressed by homogenous vectors, then the mapping can be represented as a linear relationship between them. Such mathematical model can be written as a linear combination of the external (position and orientation) and internal (focal length and sensor size) camera parameters.

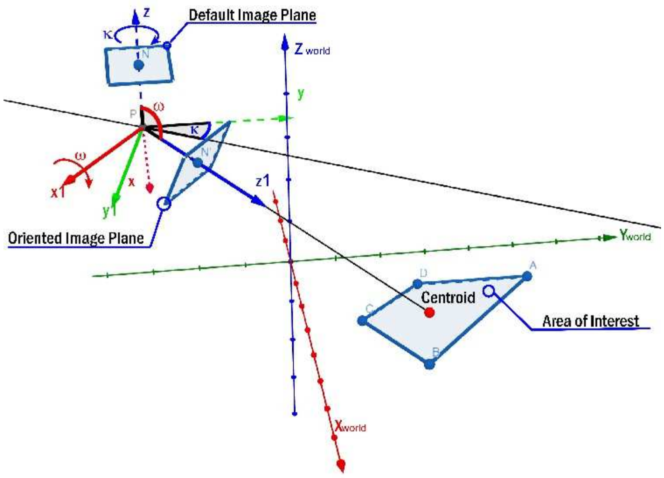

Fig. 1 – The default image plane is centered on a generic DSM vertex and the camera reference system is oriented parallel to the world one. In order to point the centroid of the area of interest, two rotations shall be performed: around the z axis first and the x_1 axis then.

The optical centre moves through the DSM vertexes and assumes all the possible positions on the coast surface, while the orientation parameters are unknown. The first step is to define the camera position on the DMS; afterwards, the camera orientation parameters can be obtained supposing that the optical axis points the area of interest. Such operation can be carried out by constraining the optical axis on the line connecting the perspective and the centroid of the area of interest. This condition is realized performing two rotations: the first one is made around the "z" camera axis to bring the

"y" camera axis along the vertical plane passing through the perspective centre and the centroid of the area of interest. The second rotation is then performed around the new "x_1" axis to bring the optical axis towards the centroid of the area of interest (figure 1).
Considering κ e ω as the rotation angles around the **z** and $\mathbf{x_1}$ axis respectively: the rotation matrix ***R*** can be computed as follow:

$$\mathbf{R}=\begin{pmatrix}1 & 0 & 0\\ 0 & \cos\omega & \sin\omega\\ 0 & -\sin\omega & \cos\omega\end{pmatrix}\begin{pmatrix}\cos\kappa & \sin\kappa & 0\\ -\sin\kappa & \cos\kappa & 0\\ 0 & 0 & 1\end{pmatrix} \quad (1)$$

The considered rotations hold the wide side of the camera horizontal. The described approach allows to optimize the coverage of the area of interest in this case study. Other cases could require an additional rotation around the optical axis as well.
The intrinsic parameters matrix can be described through the calibration matrix ***K***:

$$\mathbf{K}=\begin{pmatrix}f & 0 & x_0\\ 0 & f & y_0\\ 0 & 0 & 1\end{pmatrix} \quad (2)$$

where f is the focal length and x_0 and y_0 are the image coordinates of the principal point (i.e., the intersection between the optical axis and the sensor plane). The calibration matrix represents the mathematical model of the camera and the features of its internal geometry.
The mapping relationship between the camera coordinates and the 3D coordinates can be represented by the projection matrix **P,** obtained as follows:

$$\mathbf{P=K \cdot R \cdot [I|-C]} \quad (3)$$

This matrix allows to define the relationship between the 3D space coordinates and the 2D image coordinates expressed as homogenous vectors:

$$\mathbf{[x\ |1]^T=P \cdot [X|1]^T} \quad (6)$$

For this case study, the Earth curvature can be neglected, being the dimensions of the area of interest quite small; therefore, the sea surface is here assumed as a Euclidean plane. This condition greatly simplifies the projection matrix since the Z coordinate can be set to zero.

$$\begin{bmatrix}x\\ y\\ 1\end{bmatrix}=[p_1 \quad p_2 \quad p_3 \quad p_4]\cdot\begin{bmatrix}X\\ Y\\ Z\\ 1\end{bmatrix} \quad (5)$$

where $\mathbf{p}_i$ is a column vector representing the projection matrix. The Equation (5) can be rewritten as (6):

$$\begin{bmatrix}x\\ y\\ 1\end{bmatrix}=[p_1 \quad p_2 \quad p_4]\cdot\begin{bmatrix}X\\ Y\\ 1\end{bmatrix}=H\cdot\begin{bmatrix}X\\ Y\\ 1\end{bmatrix} \quad (6)$$

The matrix **H** (6) is a 3x3 square matrix with full rank. Such matrix is known as homography matrix, and it maps the coordinates from the sea surface plane to the image plane and reverse.

III. Discussion & Results

A. *Virtual Enviroment Setup*

The inspection has been conducted in a simulated environment, setting a virtual camera with a standard High-Definition resolution of 1920x1080 pixel and an equivalent focal length of 60 mm, with the principal point being at the center of the image plane. In this preliminary study, the image distortion normally introduced by the physical lens has been neglected.
A DSM obtained through aerial LiDAR (Light Detection And Ranging) data has been used as a 3D model for the coastal area of interest. The raw data processing was performed using the last return of the laser pulse. The result can be represented as a dense gridded points cloud with a cell dimension 1-by-1 meter linked to the reference frame ETRF89 (Figure 2).

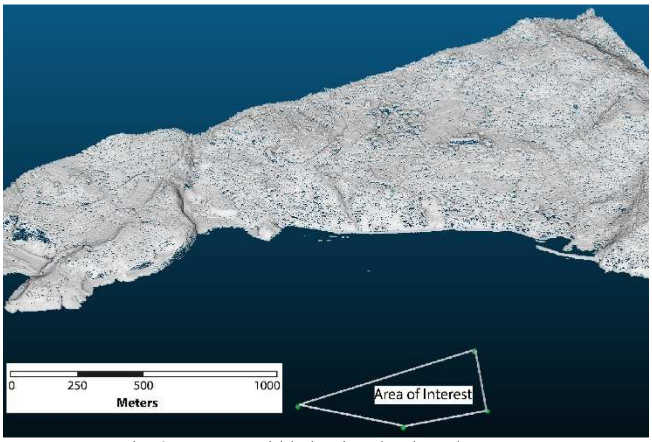

Fig. 2 – Dense gridded point cloud used as DSM

A specific algorithm was implemented in the MatLab® environment with the aim of moving the camera center from a point of the DSM to another and to further place the optical axis in the direction of the centroid of the area of interest.

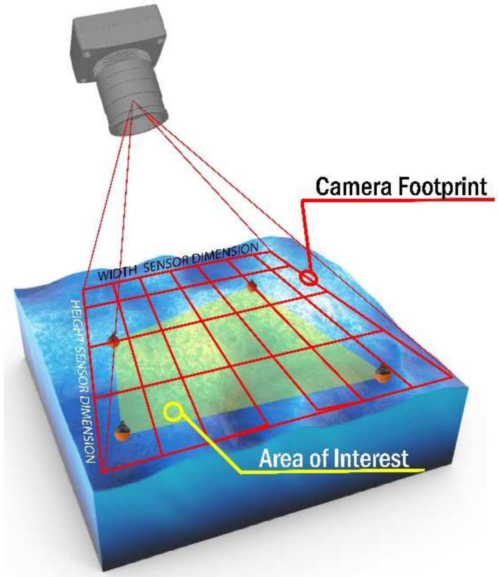

Fig. 3 – A generic camera footprint and the reprojection of the sensor pixel grid on the sea surface.

Finally, the projection and the corresponding homography matrixes were computed for each point of the DSM.

The projection matrix is then used to determine the image coordinates of the area of interest vertexes, while the homography matrix is employed to reproject the sensor pixels grid which covers the area of interest on the sea surface (Figure 3). The obtained result is a grid on the sea surface composed by cells with irregular shape (consequently an irregular GSD).

The figure 4 shows a generic camera, oriented according to the developed approach as illustrated in the previous section. Moreover, in cyan is represented part of the camera sensor on projected the sea surface. The cropping was performed to completely cover the area of interest. As shown in figure 4, the width sensor dimension is smaller than the height one; both dimensions increase their size as the distance between the projected point and camera center increase.

The inspection is then performed on the GSD size to identify the mean covered area by a pixel and the mean of the two GSD dimensions. Specifically, in this work, the assessment focused on the GSD mean area (approach n°1) and the mean GSD height dimension (approach n°2).

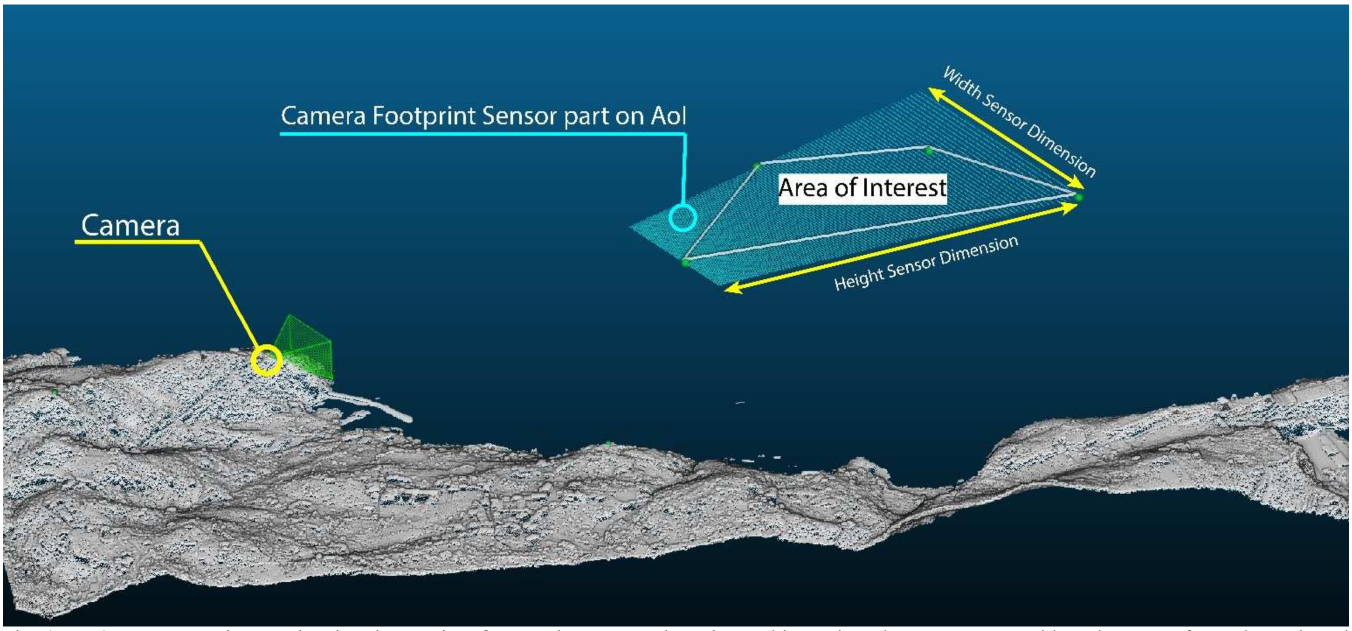

Fig. 4 – A 3D representation, on the virtual scenario, of a generic camera orientation and its projected camera sensor grid on the sea surface. The projected area was cropped to cover the entire Area of Interest

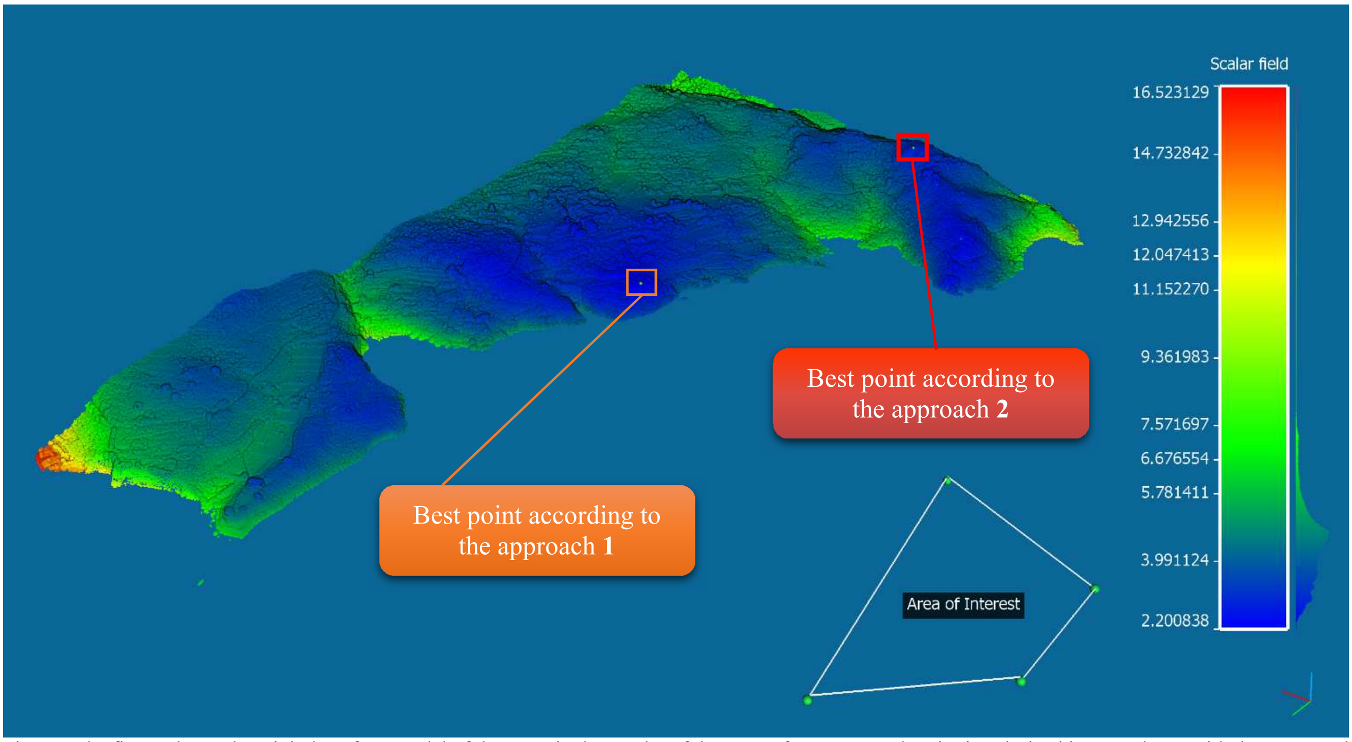

Fig. 5 – The figure shows the Digital Surface Model of the coast in the nearby of the Area of Interest. Each point is colorized in accordance with the computed mean area of the GSD. The values of the scalar fields are expressed in square meters.

B. Results

The grid size and the mean GSD area is computed for each point of the DSM. These parameters allow to colorize the 3D cloud point according to the obtained results. Figure 5 shows the colorization of the DSM of the coast in which the color scale field is based on the average area covered by a pixel of the defined virtual camera. The resulting-colored map allows to detect which area of the coast is suitable for installing the camera. Figure 5 shows the zones which provide the smallest and the largest GSD areas colorized respectively in blue and red. Furthermore, two points were detected on the DSM, which minimize the mean GSD area (approach 1) and the mean height GSD dimension (approach 2). These points are the best candidates for installing a surveillance camera.

C. Discussion

The achieved results allowed to estimate the best position for the installation of a camera covering a small GSD area and minimizing the GSD height dimension in average. Although such area is a good indicator of the capability to detect a target and its speed, the shape of GSD assumes an important role as well. Indeed, it must be considered that the height dimension could become 10-20 times larger than the width one, thus generating two different spatial resolutions. Since the capability to detect a target and its speed is strongly related to the spatial resolution, further analysis should be conducted to inspect the range of routes which could provide an adequate accuracy. In this work just two different criteria were used for inspecting the spatial resolution of the camera footprint. Of course, other approaches can be introduced to evaluate the camera best position, although the coast morphology would provide similar results.

Another issue which should be considered to improve the results is related to the visibility. In fact, the presence of buildings and other artificial structures could partially obstruct the view of the area of interest, thus making the study of the visibility from a generic DSM point of particular importance.

IV. Conclusion and Future Developments

This work deals with the problem of monitoring the nautical traffic in coastal areas, which constitute a challenging task especially during the summer. In particular, an automatic approach is here proposed to strategically place a camera on the coast of the area of interest, from which tracking the vessels and their speeds. The study has been conducted in the MPA of 'Punta Campanella', on the coast of the Campania Region, Italy.

Preliminary results demonstrate the validity of this method, showing very promising scope for improvement. Nevertheless, in this work, the internal camera parameters (i.e. focal length, sensor pixel size and distortion coefficient) remain unchanged; further future developments of the methodology could regard these parameters. The study could provide the best location of the camera as well as the best focal length and pixel size for obtaining a sure detection of a known size boat.

Finally, further works and crossed inspections could verify if the presence of obstructions in the camera field of view has an impact on the overall results.

References

[1] Van Westrenen, Fulko; Praetorius, Gesa. Maritime traffic management: a need for central coordination?. Cognition, technology & work, 2014, 16.1: 59-70.

[2] Iphar, C., Napoli, A., Ray, C., Alincourt, E., & Brosset, D. (2016, September). Risk Analysis of falsified Automatic Identification System for the improvement of maritime traffic safety. In *Proceedings of the ESREL 2016 Conference* (pp. 606-613). Taylor & Francis.

[3] Zhen, R., Riveiro, M., & Jin, Y. (2017). A novel analytic framework of real-time multi-vessel collision risk assessment for maritime traffic surveillance. *Ocean Engineering*, *145*, 492-501.

[4] Madariaga, E., Sánchez, L., Pérez-Labajos, C. A., Ortega, A., Blanco, B., & Oria, J. M. (2014). NCAGS a tool for protection of maritime traffic. In *Developments in Maritime Transportation and Exploitation of Sea Resources-Proceedings of IMAM 2013, 15th International Congress of the International Maritime Association of the Mediterranean* (Vol. 2, pp. 727-733).

[5] Conventions on the International Regulations for Preventing Collision at Sea (COLREGs), The International Maritime Organization (IMO) (1972)

[6] SOLAS1974.International Convention for the Safety of Life at Sea Chapter V,IMO Ammended 2018.

[7] Pietrzykowski, Z., & Magaj, J. (2017). Ship domain as a safety criterion in a precautionary area of traffic separation scheme. TransNav: International Journal on Marine Navigation and Safety of Sea Transportation, 11(1).

[8] Mansson, Joakim Trygg, Margareta Lutzhoft, and Ben Brooks. "Joint activity in the maritime traffic system: perceptions of ship masters, maritime pilots, tug masters, and vessel traffic service operators." *The Journal of Navigation* 70.3 (2017): 547-560.

[9] Pietrzykowski, Z., & Narekiewicz, M. (2002). Implementation of marine regulations in decision support systems for vessel traffic services. *WIT Transactions on The Built Environment*, *62*.

[10] Young, W. (1994). What Are Vessel Traffic Services and What Can They Really Do?. *NAVIGATION, Journal of the Institute of Navigation*, *41*(1), 31-56.

[11] Sluiman, I. F., & de Koning, H. (2010). Naval vessel traffic services: Enhancing the safety of merchant shipping in maritime security operations. *Naval War College Review*, *63*(3), 123-138.

[12] Seta, H., Oki, M., Usui, H., & Sakaide, M. (2010). Marine Traffic Analysis of Three Major Bays: Ship Handling Difficulty of Ship Equipped with AIS. *The Journal of Japan Institute of Navigation*, *123*.

[13] Ahlberg, E., & Danielsson, J. (2016). *Handling and Analyzing Marine Traffic Data* (Master's thesis).

[14] Ministero delle Infrastrutture e dei Trasporti (2018). *Rapporto sui sinistri marittimi e sugli infortuni a bordo alle navi.* Report of the Italian Department for Transport and Navigation.

[15] Widmer WM, Underwood AJ "Factors affecting traffic and anchoring patterns of recreational boats in Sydney Harbour, Australia". Landscape Urban Plan 66: 173–183, 2004.

[16] Bracciali, Claudia, Daniela Campobello, Cristina Giacoma, Gianluca Sara. "Effects of nautical traffic and noise on foraging patterns of Mediterranean damselfish (Chromis chromis)." PloS one 7, no. 7 (2012): https://doi.org/10.1371/journal.pone.0040582.

[17] Bilkovic, D. M., Mitchell, M. M., Davis, J., Herman, J., Andrews, E., King, A., ... & Dixon, R. L. (2019). Defining boat wake impacts on shoreline stability toward management and policy solutions. *Ocean & Coastal Management*, *182*, 104945.

[18] Manis, J. E., Garvis, S. K., Jachec, S. M., & Walters, L. J. (2015). Wave attenuation experiments over living shorelines over time: a wave tank study to assess recreational boating pressures. *Journal of coastal conservation*, *19*(1), 1-11.

[19] Potmesil, M., & Chakravarty, I. (1982). Synthetic image generation with a lens and aperture camera model. *ACM Transactions on Graphics (TOG)*, *1*(2), 85-108.

[20] Li, H., Adams, B., Guibas, L. J., & Pauly, M. (2009). Robust single-view geometry and motion reconstruction. *ACM Transactions on Graphics (ToG)*, *28*(5), 1-10.

[21] A. Criminisi, "Single-view metrology: Algorithms and applications", *Proceedings of the 24th DAGM Symposium on Pattern Recognition*, pp. 224-239, 2002.

[22] Chen, H. T., Tsai, W. J., Lee, S. Y., & Yu, J. Y. (2012). Ball tracking and 3D trajectory approximation with applications to tactics analysis from single-camera volleyball sequences. *Multimedia Tools and Applications*, *60*(3), 641-667.

[23] Honey, S., & Milnes, K. (2013). The annotated america's cup. *IEEE Spectrum*, *50*(9), 36-42.

[24] Gao, Q., Wang, H., & Wang, J. (2012). A single camera volumetric particle image velocimetry and its application. *Science China Technological Sciences*, *55*(9), 2501-2510.

[25] Pesce, V., Opromolla, R., Sarno, S., Lavagna, M., & Grassi, M. (2019). Autonomous relative navigation around uncooperative spacecraft based on a single camera. *Aerospace Science and Technology*, *84*, 1070-1080.

[26] Gaglione, S., Del Pizzo, S., Troisi, S., & Angrisano, A. (2018). POSITION ACCURACY ANALYSIS OF A ROBUST VISION-BASED NAVIGATION SYSTEM. *International Archives of the Photogrammetry, Remote Sensing & Spatial Information Sciences*, *42*(2).

[27] Sazdovski, V., Silson, P. M., & Tsourdos, A. (2010, July). Attitude determination from single camera vector observations. In *2010 5th IEEE International Conference Intelligent Systems* (pp. 49-54). IEEE.

[28] Del Pizzo, S., Gaglione, S., Angrisano, A., Salvi, G., & Troisi, S. (2018). Reliable vessel attitude estimation by wide angle camera. *Measurement*, *127*, 314-324.

[29] Fu, K., Peng, J., He, Q., & Zhang, H. (2021). Single image 3D object reconstruction based on deep learning: A review. *Multimedia Tools and Applications*, *80*(1), 463-498.

R. Hartley and A. Zisserman, Multiple View Geometry in Computer Vision, Cambridge University Press, 2004, ISBN 0521540518.